SDU
University of Southern Denmark

Gradient corrections to false vacuum decay in the gauge sector

based on Phys. Rev. D102, 085001

Juan S. Cruz

together with:

B. Garbrecht, W. Ai and C. Tamarit

Det Naturvidenskabelige Fakultet

CP^3-Origins

30th Nordic Network Meeting on “Strings, Fields and Branes”- 23rd of Nov. 2021

1. Motivation

Current measurements of the masses of the Higgs and the top quark, place our universe in a metastable region of the Higgs field potential

[Degrassi et al., 2012]
[Buttazzo et al., 2013]

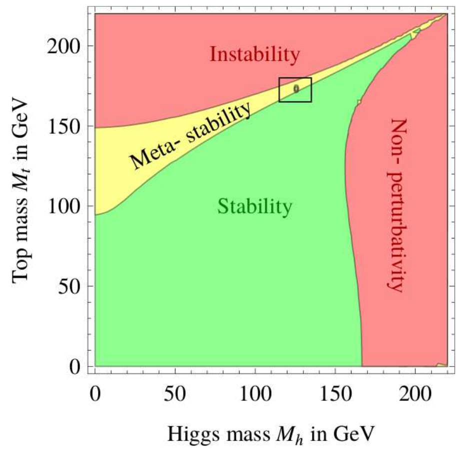

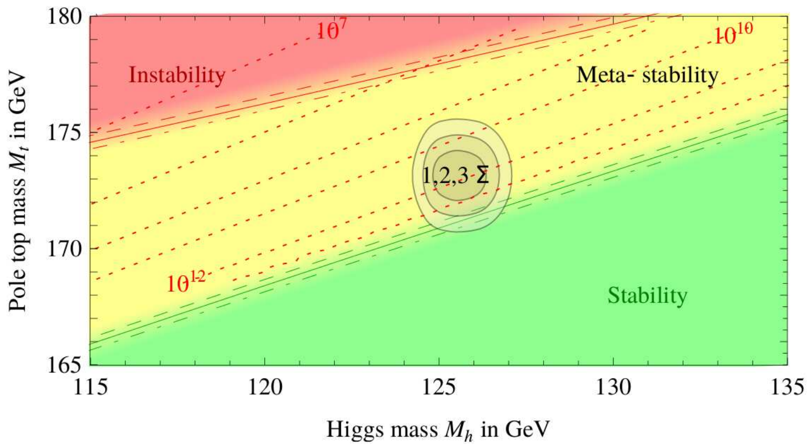

The metastability region is characterized by more than one local minimum allowing for tunneling phenomena associated with regions of different phases.

1. Motivation

Current measurements of the masses of the Higgs and the top quark, place our universe in a metastable region of the Higgs field potential

[Degrassi et al., 2012]
[Buttazzo et al., 2013]

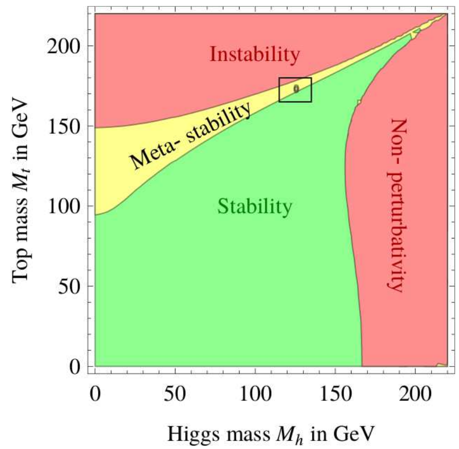

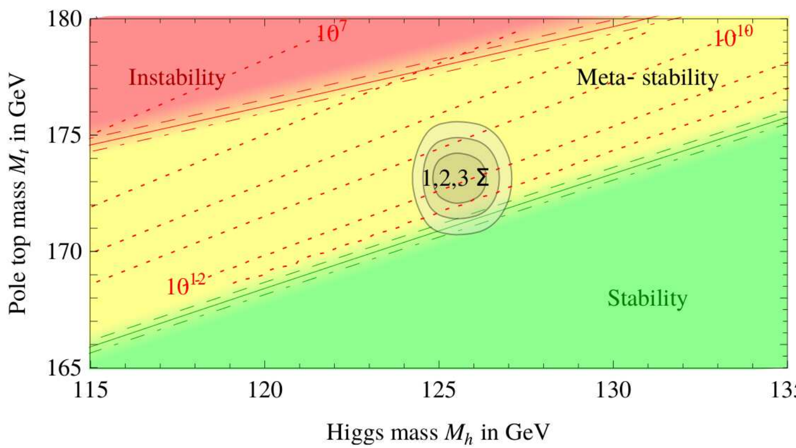

The metastability region is characterized by more than one local minimum allowing for tunneling phenomena associated with regions of different phases.

[Coleman, 1977]
[Callan and Coleman, 1977]

1. Motivation

Current measurements of the masses of the Higgs and the top quark, place our universe in a metastable region of the Higgs field potential

[Degrassi et al., 2012]
[Buttazzo et al., 2013]

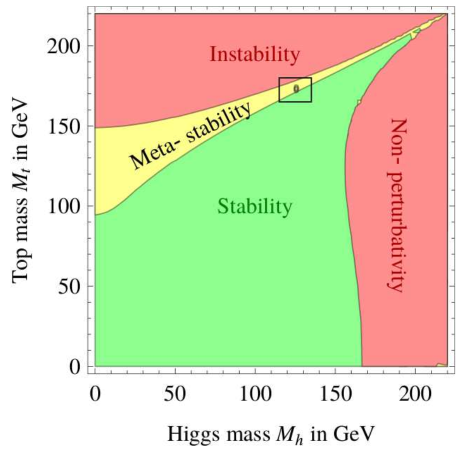

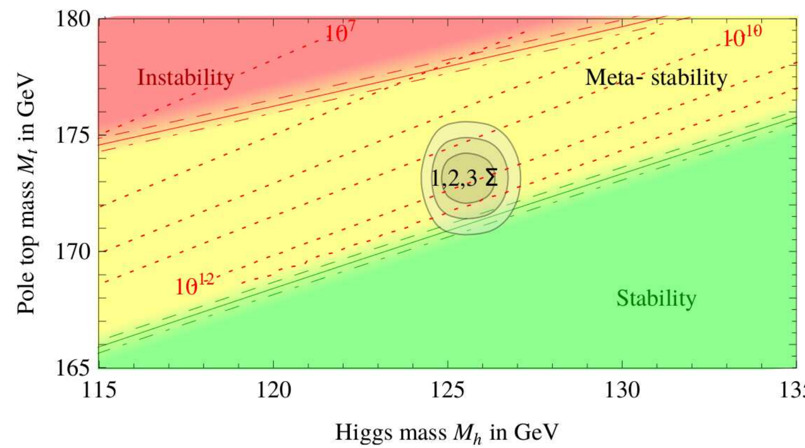

The metastability region is characterized by more than one local minimum allowing for tunneling phenomena associated with regions of different phases.

[Coleman, 1977]
[Callan and Coleman, 1977]

Tachyonic regions and gradient effects are not well described by a Coleman-Weinberg potential and new methods must be sought.

2. How is true vacuum produced?

Bubble nucleation

A non-homogeneous background called the bounce, denoted by $\varphi_b(r)$, is used subject to a scalar potential able to nucleate bubbles.

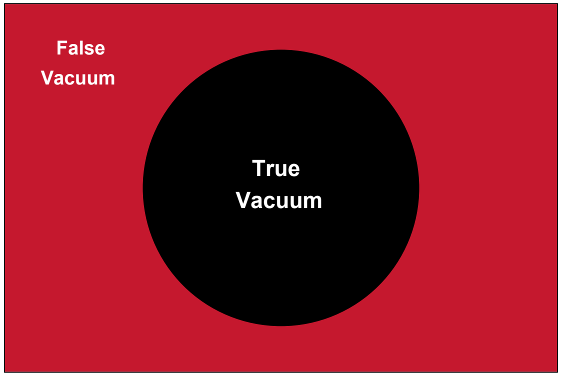

2. How is true vacuum produced?

Bubble nucleation

A non-homogeneous background called the bounce, denoted by $\varphi_b(r)$, is used subject to a scalar potential able to nucleate bubbles.

[Lee and Weinberg, 1986]
[Andreassen et al., 2017]

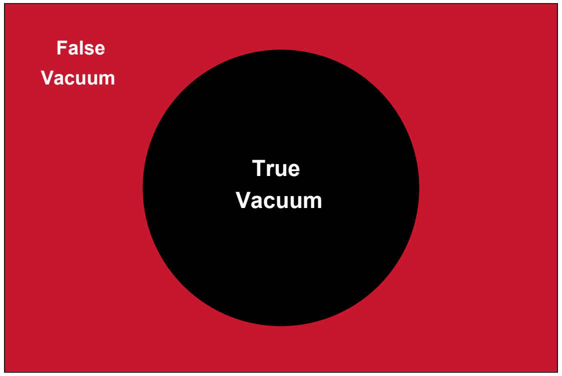

Gradients play a role in tunneling situations, which most treatments do not account for.

Different cases such as other geometries, EW phase transition and scale invariant potentials, coupling to gravity, etc. have been treated

[Baacke, 1990], [Baacke and Junker, 1994], [Sürig, 1998], [Garbrecht and Millington, 2015], [Garbrecht and Millington, 2017], [Ai et al., 2018].

3.The Vanilla Decay Rate

The ground state

Denote the constant field configuration corresponding to the false vacuum by φ_+.

The vacuum-to-vacuum transition amplitude

$$\langle\varphi_+|e^{-HT/\hbar}|\varphi_+\rangle = \sum_n \mathrm{e}^{-E_n T/\hbar}\langle\varphi_+|n\rangle\langle n|\varphi_+\rangle \sim e^{-E_0 T/\hbar}\langle\varphi_+|0\rangle\langle 0|\varphi_+\rangle$$

projects out the lowest energy state at large imaginary times.

3.The Vanilla Decay Rate

The ground state

Denote the constant field configuration corresponding to the false vacuum by φ_+.

The vacuum-to-vacuum transition amplitude

$$\langle\varphi_+|e^{-HT/\hbar}|\varphi_+\rangle = \sum_n \mathrm{e}^{-E_n T/\hbar}\langle\varphi_+|n\rangle\langle n|\varphi_+\rangle \sim e^{-E_0 T/\hbar}\langle\varphi_+|0\rangle\langle 0|\varphi_+\rangle$$

projects out the lowest energy state at large imaginary times.

The Semi-classical approach

Such amplitude can also be written in terms of the partition function

$$\langle\varphi_+|e^{-HT/\hbar}|\varphi_+\rangle = Z[0] = \mathcal{N}\int \mathscr{D}\phi\, e^{-S_E[\phi]} \sim e^{-S_E(\varphi_b)}.$$

The energy of the ground state may have an imaginary part which relates to the decay rate

$$\frac{\gamma}{V} = -\frac{2}{\hbar}\mathfrak{Im}\lim_{T\to\infty}\frac{\ln Z[0]}{T}$$

4. Previous Studies and Improvements

Effective action in the standard model

Some have investigated conditions for vacuum stability.

Others assume a metastable situation and compute the decay rates to use as bounds

[Hung, 1979], [Cabibbo et al., 1979]
[Isidori et al., 2001],
[Andreassen et al., 2015].

4. Previous Studies and Improvements

Effective action in the standard model

Some have investigated conditions for vacuum stability.

Others assume a metastable situation and compute the decay rates to use as bounds

[Hung, 1979], [Cabibbo et al., 1979]
[Isidori et al., 2001],
[Andreassen et al., 2015].

4. Previous Studies and Improvements

Effective action in the standard model

Some have investigated conditions for vacuum stability.

Others assume a metastable situation and compute the decay rates to use as bounds

[Hung, 1979], [Cabibbo et al., 1979]
[Isidori et al., 2001],
[Andreassen et al., 2015].

4. Previous Studies and Improvements

Effective action in the standard model

Some have investigated conditions for vacuum stability.

Others assume a metastable situation and compute the decay rates to use as bounds

[Hung, 1979], [Cabibbo et al., 1979]
[Isidori et al., 2001],
[Andreassen et al., 2015].

Including higher loop order effects

There is a relation between the decay rate, γ, and the effective action, $\Gamma^{(n)}$, given by

[Garbrecht and Millington, 2015]

$$\gamma/V = 2\left|\mathfrak{Im}\, e^{-\Gamma^{(n)}[\varphi^{(n)}]/\hbar}\right|/VT$$

In our study

$$\Gamma_{\mathrm{sc}}[\varphi^{(1)}] = B + \hbar B^{(1)} + \hbar^2 B^{(2)}$$

5. Our toy model for a $U(1)$

Consider the following Lagrangian in Euclidean space-time

$$\mathscr{L}_E = \frac{1}{4} F_{\mu\nu} F_{\mu\nu} + (D_\mu \phi)^* (D_\mu \phi) + U(\phi^* \phi) + \mathscr{L}_{\text{G.F.}} + \mathscr{L}_{\text{ghost}},$$

where

$$U(\phi^*\phi) = \alpha(\phi^*\phi) + \lambda(\phi^*\phi)^2 + \lambda_6(\phi^*\phi)^3,$$

$$\mathscr{L}_{\text{G.F.}} = \frac{1}{2\xi}(\partial_\mu A_\mu - \zeta g \phi G)^2,$$

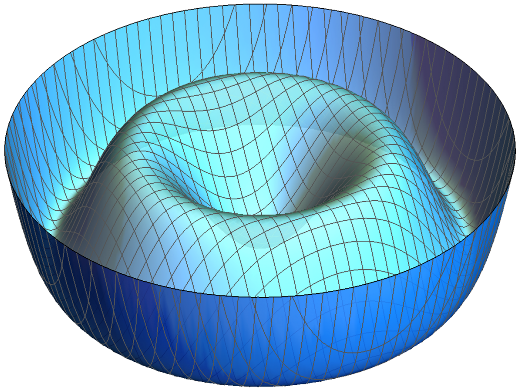

and leads to the generating functional

$$Z[J, K_\mu, \bar{\psi}, \psi] = \int \mathscr{D}[\phi, A_\mu, \eta, \bar{\eta}] \exp\Bigg(-\frac{1}{\hbar} \int \mathrm{d}^4 x \, \Big[\mathscr{L}_E - J(x)\phi(x) - K_\mu(x) A_\mu(x) - \bar{\psi}(x)\eta(x) - \bar{\eta}(x)\psi(x) \Big] \Bigg).$$

6. Self-consistent Green's function method

6. Self-consistent Green's function method

1. Obtain the vacua-interpolating background, φ_b, the bounce.

6. Self-consistent Green's function method

1. Obtain the vacua-interpolating background, φ_b, the bounce.
2. Solve for the tree-level Green's functions in position space for the propagators of the fluctuations

$$\left.\frac{\delta^2 S}{\delta\Phi(x)\delta\Phi(z)}\right|_{\phi=\varphi_b} G(\varphi_b; z, y) = \delta^{(4)}(x-y).$$

6. Self-consistent Green's function method

1. Obtain the vacua-interpolating background, φ_b, the bounce.
2. Solve for the tree-level Green's functions in position space for the propagators of the fluctuations
$$\left.\frac{\delta^2 S}{\delta\Phi(x)\delta\Phi(z)}\right|_{\phi=\varphi_b} G(\varphi_b;z,y) = \delta^{(4)}(x-y).$$
3. Compute the "$\log\det$" terms from the 1-PI effective action $\Gamma^{(1)}[\varphi_b]$.

6. Self-consistent Green's function method

1. Obtain the vacua-interpolating background, φ_b, the bounce.
2. Solve for the tree-level Green's functions in position space for the propagators of the fluctuations

$$\frac{\delta^2 S}{\delta\Phi(x)\delta\Phi(z)}\bigg|_{\phi=\varphi_b} G(\varphi_b; z, y) = \delta^{(4)}(x-y).$$

3. Compute the "$\log\det$" terms from the 1-PI effective action $\Gamma^{(1)}[\varphi_b]$.
4. The tadpole function for a field ϕ on the background φ_b,

$$\Pi(\varphi_b; x)\varphi_b(x) = \frac{\delta}{\delta\varphi(x)}\log\frac{\det M^{-1}_{\varphi_b}[\varphi(x)]}{\det M^{-1}_{\varphi_b}[0]}$$

gives the corrections to the bounce, $\delta\varphi$, according to

$$-\partial_z^2\delta\varphi(x) + U'(\varphi_b(x)+\delta\varphi(x)) + \hbar\Pi(\varphi_b; x)\varphi_b(x) = 0$$

6. Self-consistent Green's function method

1. Obtain the vacua-interpolating background, φ_b, the bounce.
2. Solve for the tree-level Green's functions in position space for the propagators of the fluctuations
$$\left.\frac{\delta^2 S}{\delta\Phi(x)\delta\Phi(z)}\right|_{\phi=\varphi_b} G(\varphi_b; z, y) = \delta^{(4)}(x-y).$$
3. Compute the "$\log\det$" terms from the 1-PI effective action $\Gamma^{(1)}[\varphi_b]$.
4. The tadpole function for a field ϕ on the background φ_b,
$$\Pi(\varphi_b; x)\varphi_b(x) = \frac{\delta}{\delta\varphi(x)} \log \frac{\det M^{-1}_{\varphi_b}[\varphi(x)]}{\det M^{-1}_{\varphi_b}[0]}$$
gives the corrections to the bounce, $\delta\varphi$, according to
$$-\partial_z^2 \delta\varphi(x) + U'(\varphi_b(x) + \delta\varphi(x)) + \hbar\Pi(\varphi_b; x)\varphi_b(x) = 0$$
5. Substituting $\delta\varphi$ back into the action yields quadratic corrections to the decay rate.

7. Wait, what is bouncing here?

The field configuration $\varphi_b(r)$ is obtained from the classical e.o.m. by looking at $O(4)$ invariant solutions connecting the minima.

7. Wait, what is bouncing here?

The field configuration $\varphi_b(r)$ is obtained from the classical e.o.m. by looking at $O(4)$ invariant solutions connecting the minima.

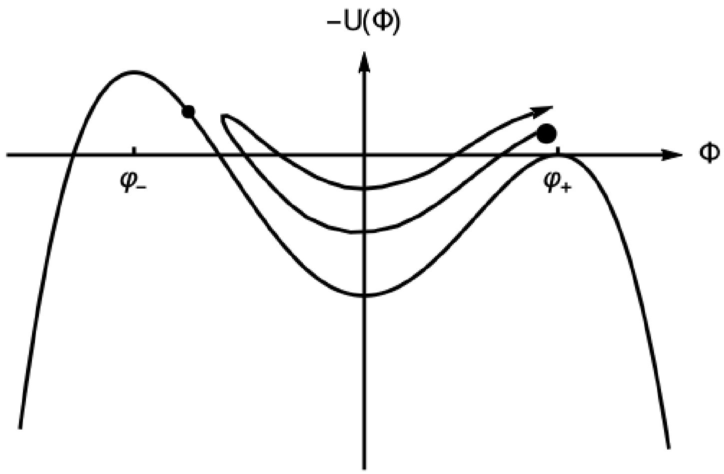

7. Wait, what is bouncing here?

The field configuration $\varphi_b(r)$ is obtained from the classical e.o.m. by looking at $O(4)$ invariant solutions connecting the minima.

In a thin wall approximation the dissipative term is ignored, with $r^2 = \mathbf{x}^2 + x_4^2$ one has:

$$-\frac{\mathrm{d}^2\varphi}{\mathrm{d}r^2} - \frac{3}{r}\frac{\mathrm{d}\varphi}{\mathrm{d}r} + U'(\varphi) = 0,$$

alternatively in Hyper-spherical harmonics' terms we keep the lower angular momentum harmonics.

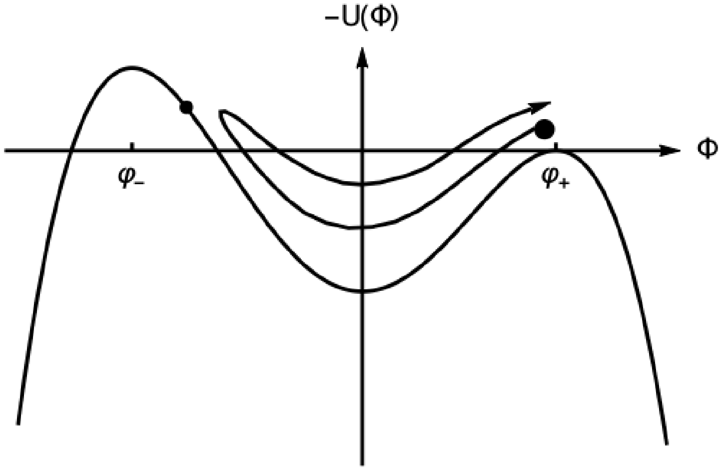

7. Wait, what is bouncing here?

The field configuration $\varphi_b(r)$ is obtained from the classical e.o.m. by looking at $O(4)$ invariant solutions connecting the minima.

In a thin wall approximation the dissipative term is ignored, with $r^2 = \mathbf{x}^2 + x_4^2$ one has:

$$-\frac{\mathrm{d}^2\varphi}{\mathrm{d}r^2} - \frac{3}{r}\frac{\mathrm{d}\varphi}{\mathrm{d}r} + U'(\varphi) = 0,$$

alternatively in Hyper-spherical harmonics' terms we keep the lower angular momentum harmonics.

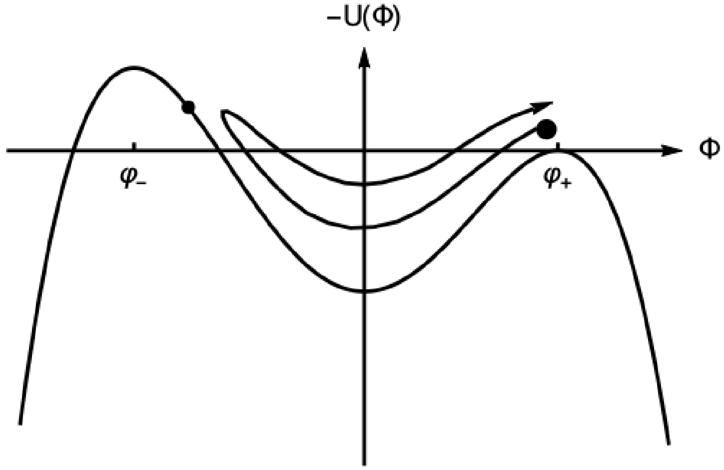

We perform a semi-classical expansion for the theory by expanding around φ_b, e.g. making the substitution:

$$\phi = \frac{1}{\sqrt{2}}(\varphi_b + \hat{\Phi} + iG).$$

8. 1-PI Effective action

The computation of the 1-PI effective action formally gives the expression,

$$\Gamma^{(1)}[\varphi^{(1)}] = S[\varphi^{(1)}] + \frac{\hbar}{2}\log\frac{\det \mathscr{M}^{-1}_{\hat{\Phi}}(\varphi^{(1)})}{\det \mathscr{M}^{-1}_{\hat{\Phi}}(0)} + \frac{\hbar}{2}\log\frac{\det \mathscr{M}^{-1}_{(A_\mu,G)}(\varphi^{(1)})}{\det \mathscr{M}^{-1}_{(A_\mu,G)}(0)} - \hbar\log\frac{\det \mathscr{M}^{-1}_{(\bar{\eta},\eta)}(\varphi^{(1)})}{\det \mathscr{M}^{-1}_{(\bar{\eta},\eta)}(0)},$$

8. 1-PI Effective action

The computation of the 1-PI effective action formally gives the expression,

$$\Gamma^{(1)}[\varphi^{(1)}] = S[\varphi^{(1)}] + \frac{\hbar}{2}\log\frac{\det\mathscr{M}^{-1}_{\hat{\Phi}}(\varphi^{(1)})}{\det\mathscr{M}^{-1}_{\hat{\Phi}}(0)} + \frac{\hbar}{2}\log\frac{\det\mathscr{M}^{-1}_{(A_\mu,G)}(\varphi^{(1)})}{\det\mathscr{M}^{-1}_{(A_\mu,G)}(0)} - \hbar\log\frac{\det\mathscr{M}^{-1}_{(\bar{\eta},\eta)}(\varphi^{(1)})}{\det\mathscr{M}^{-1}_{(\bar{\eta},\eta)}(0)},$$

where the operators are:

$$\mathscr{M}^{-1}_{\hat{\Phi}}(\varphi^{(1)}) = -\Delta + \alpha + 3\lambda\,(\varphi^{(1)})^2 + \frac{15\,\lambda_6}{4}(\varphi^{(1)})^4\,,$$

$$\mathscr{M}^{-1}_{(A_\mu,G)}(\varphi^{(1)}) = \begin{pmatrix} (-\Delta + g^2(\varphi^{(1)})^2)\,\delta_{\mu\nu} + \frac{\xi-1}{\xi}\partial_\mu\partial_\nu & \left(\frac{\zeta+\xi}{\xi}\right)g\,(\partial_\mu\varphi^{(1)}) + \left(\frac{\zeta-\xi}{\xi}\right)g\,\varphi^{(1)}\,\partial_\mu \\ 2\,g\,(\partial_\nu\varphi^{(1)}) + \left(\frac{\xi-\zeta}{\xi}\right)g\,\varphi^{(1)}\,\partial_\nu & -\Delta + \alpha + \lambda\,(\varphi^{(1)})^2 + \frac{3\lambda_6}{4}(\varphi^{(1)})^4 + \frac{\zeta^2}{\xi}g^2(\varphi^{(1)})^2 \end{pmatrix},$$

$$\mathscr{M}^{-1}_{(\bar{\eta},\eta)}(\varphi^{(1)}) = -\Delta + \zeta\,g^2\,(\varphi^{(1)})^2.$$

and $\varphi^{(1)}$ contains the quantum fluctuations.

8. 1-PI Effective action

The computation of the 1-PI effective action formally gives the expression,

$$\Gamma^{(1)}[\varphi^{(1)}] = S[\varphi^{(1)}] + \frac{\hbar}{2}\log\frac{\det\mathscr{M}^{-1}_{\hat{\Phi}}(\varphi^{(1)})}{\det\mathscr{M}^{-1}_{\hat{\Phi}}(0)} + \frac{\hbar}{2}\log\frac{\det\mathscr{M}^{-1}_{(A_\mu,G)}(\varphi^{(1)})}{\det\mathscr{M}^{-1}_{(A_\mu,G)}(0)} - \hbar\log\frac{\det\mathscr{M}^{-1}_{(\bar{\eta},\eta)}(\varphi^{(1)})}{\det\mathscr{M}^{-1}_{(\bar{\eta},\eta)}(0)},$$

where the operators are:

$$\mathscr{M}^{-1}_{\hat{\Phi}}(\varphi^{(1)}) = -\Delta + \alpha + 3\lambda\,(\varphi^{(1)})^2 + \frac{15\lambda_6}{4}(\varphi^{(1)})^4\,,$$

$$\mathscr{M}^{-1}_{(A_\mu,G)}(\varphi^{(1)}) = \begin{pmatrix} (-\Delta + g^2(\varphi^{(1)})^2)\,\delta_{\mu\nu} + \frac{\xi-1}{\xi}\partial_\mu\partial_\nu & \left(\frac{\zeta+\xi}{\xi}\right)g\,(\partial_\mu\varphi^{(1)}) + \left(\frac{\zeta-\xi}{\xi}\right)g\,\varphi^{(1)}\,\partial_\mu \\ 2g\,(\partial_\nu\varphi^{(1)}) + \left(\frac{\xi-\zeta}{\xi}\right)g\,\varphi^{(1)}\,\partial_\nu & -\Delta + \alpha + \lambda\,(\varphi^{(1)})^2 + \frac{3\lambda_6}{4}(\varphi^{(1)})^4 + \frac{\zeta^2}{\xi}g^2(\varphi^{(1)})^2 \end{pmatrix},$$

$$\mathscr{M}^{-1}_{(\bar{\eta},\eta)}(\varphi^{(1)}) = -\Delta + \zeta\,g^2\,(\varphi^{(1)})^2.$$

and $\varphi^{(1)}$ contains the quantum fluctuations.

8. 1-PI Effective action

The computation of the 1-PI effective action formally gives the expression,

$$\Gamma^{(1)}[\varphi^{(1)}] = S[\varphi^{(1)}] + \frac{\hbar}{2}\log\frac{\det \mathscr{M}^{-1}_{\hat{\Phi}}(\varphi^{(1)})}{\det \mathscr{M}^{-1}_{\hat{\Phi}}(0)} + \frac{\hbar}{2}\log\frac{\det \mathscr{M}^{-1}_{(A_\mu,G)}(\varphi^{(1)})}{\det \mathscr{M}^{-1}_{(A_\mu,G)}(0)} - \hbar\log\frac{\det \mathscr{M}^{-1}_{(\bar{\eta},\eta)}(\varphi^{(1)})}{\det \mathscr{M}^{-1}_{(\bar{\eta},\eta)}(0)},$$

where the operators are:

$$\mathscr{M}^{-1}_{\hat{\Phi}}(\varphi^{(1)}) = -\Delta + \alpha + 3\lambda\,(\varphi^{(1)})^2 + \frac{15\lambda_6}{4}(\varphi^{(1)})^4\,,$$

$$\mathscr{M}^{-1}_{(A_\mu,G)}(\varphi^{(1)}) = \begin{pmatrix} (-\Delta + g^2(\varphi^{(1)})^2)\,\delta_{\mu\nu} + \frac{\xi-1}{\xi}\partial_\mu\partial_\nu & \left(\frac{\zeta+\xi}{\xi}\right) g\,(\partial_\mu\varphi^{(1)}) + \left(\frac{\zeta-\xi}{\xi}\right) g\,\varphi^{(1)}\,\partial_\mu \\ 2g\,(\partial_\nu\varphi^{(1)}) + \left(\frac{\xi-\zeta}{\xi}\right) g\,\varphi^{(1)}\,\partial_\nu & -\Delta + \alpha + \lambda\,(\varphi^{(1)})^2 + \frac{3\lambda_6}{4}(\varphi^{(1)})^4 + \frac{\zeta^2}{\xi} g^2(\varphi^{(1)})^2 \end{pmatrix},$$

$$\mathscr{M}^{-1}_{(\bar{\eta},\eta)}(\varphi^{(1)}) = -\Delta + \zeta\,g^2(\varphi^{(1)})^2.$$

and $\varphi^{(1)}$ contains the quantum fluctuations.

8. 1-PI Effective action

The computation of the 1-PI effective action formally gives the expression,

$$\Gamma^{(1)}[\varphi^{(1)}] = S[\varphi^{(1)}] + \frac{\hbar}{2}\log\frac{\det\mathscr{M}^{-1}_{\hat{\Phi}}(\varphi^{(1)})}{\det\mathscr{M}^{-1}_{\hat{\Phi}}(0)} + \frac{\hbar}{2}\log\frac{\det\mathscr{M}^{-1}_{(A_\mu,G)}(\varphi^{(1)})}{\det\mathscr{M}^{-1}_{(A_\mu,G)}(0)} - \hbar\log\frac{\det\mathscr{M}^{-1}_{(\bar{\eta},\eta)}(\varphi^{(1)})}{\det\mathscr{M}^{-1}_{(\bar{\eta},\eta)}(0)},$$

where the operators are:

$$\mathscr{M}^{-1}_{\hat{\Phi}}(\varphi^{(1)}) = -\Delta + \alpha + 3\lambda(\varphi^{(1)})^2 + \frac{15\lambda_6}{4}(\varphi^{(1)})^4\,,$$

$$\mathscr{M}^{-1}_{(A_\mu,G)}(\varphi^{(1)}) = \begin{pmatrix} (-\Delta + g^2(\varphi^{(1)})^2)\,\delta_{\mu\nu} + \frac{\xi-1}{\xi}\partial_\mu\partial_\nu & \left(\frac{\zeta+\xi}{\xi}\right)g\,(\partial_\mu\varphi^{(1)}) + \left(\frac{\zeta-\xi}{\xi}\right)g\,\varphi^{(1)}\,\partial_\mu \\ 2g\,(\partial_\nu\varphi^{(1)}) + \left(\frac{\xi-\zeta}{\xi}\right)g\,\varphi^{(1)}\,\partial_\nu & -\Delta + \alpha + \lambda(\varphi^{(1)})^2 + \frac{3\lambda_6}{4}(\varphi^{(1)})^4 + \frac{\zeta^2}{\xi}g^2(\varphi^{(1)})^2 \end{pmatrix},$$

$$\mathscr{M}^{-1}_{(\bar{\eta},\eta)}(\varphi^{(1)}) = -\Delta + \zeta\,g^2(\varphi^{(1)})^2.$$

and $\varphi^{(1)}$ contains the quantum fluctuations.

Obs: When evaluated with $\varphi = \mathrm{cte}$, it reduces to the Coleman-Weinberg potential (CW) times a volume factor.

9. Simplifications and Assumptions

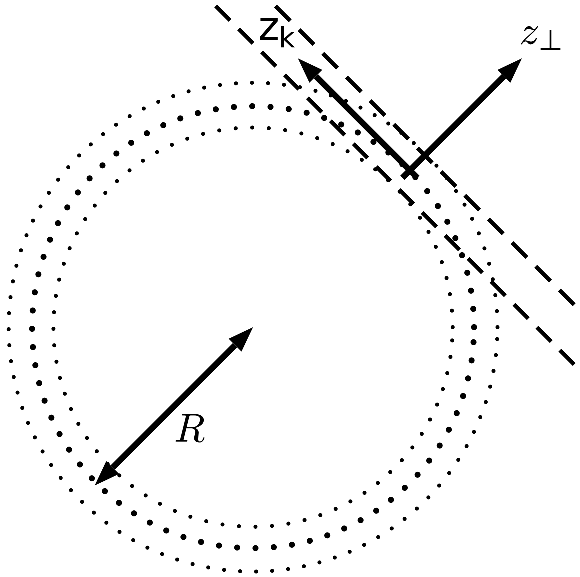

Planar Wall (3 + 1 Decomposition)

Fourier transform the tangential directions to the bubble wall. This allows us to express Green's functions as sums over 3-momentum.

9. Simplifications and Assumptions

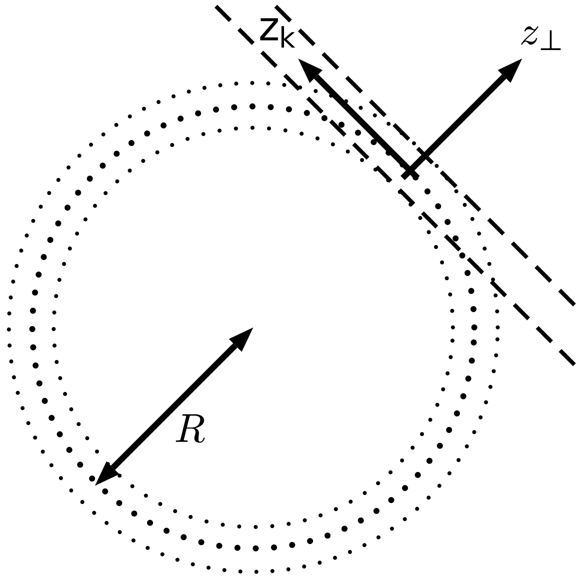

Planar Wall (3 + 1 Decomposition)

Fourier transform the tangential directions to the bubble wall. This allows us to express Green's functions as sums over 3-momentum.

Handle the easy Gauge first

$\xi = \zeta = 1$ decouples most of the components of A_μ so only A_4 and the Goldstone boson G are coupled.

10.Quest for a solution: Coupled block (A_4, G)

For small $|\mathbf{k}|$'s

For $|\mathbf{k}| \lesssim 2g\partial\varphi_b$ the gradients dominate the fluctuation operator and the system must be solved numerically using a matrix version of the R, L splitting used before.

10.Quest for a solution: Coupled block (A_4, G)

For small $|\mathbf{k}|$'s

For $|\mathbf{k}| \lesssim 2g\partial\varphi_b$ the gradients dominate the fluctuation operator and the system must be solved numerically using a matrix version of the R, L splitting used before.

For big $|\mathbf{k}|$'s

Split the operator into a diagonal and off-diagonal part,

$$\mathscr{M}^{-1}_{(A_4,G);\mathbf{k}}(\varphi_b;z) = \mathscr{M}_0^{-1}(z) + \delta\mathscr{M}^{-1}(z) = \begin{pmatrix} M_{\mathbf{k}}^{-1}(\varphi_b(z)) & 0 \\ 0 & N_{\mathbf{k}}^{-1}(\varphi_b(z)) \end{pmatrix} + \begin{pmatrix} 0 & 2g(\partial_z\varphi_b) \\ 2g(\partial_z\varphi_b) & 0 \end{pmatrix},$$

iterate over the solution to the diagonal part to include gradient corrections to all orders.

$$\mathscr{M}^{(n+1)}(z,z') = -\int \mathrm{d}z \mathscr{M}_0(z)\delta\mathscr{M}^{-1}(z)\mathscr{M}^{(n)}(z,z')$$

This simultaneously expands on the coupling g and the gradients of the background.

11. Functional determinants

We deform the operator through an auxiliary parameter s.

[Baacke and Junker, 1994].

Given a differential operator M^{-1} then its deformation is $M_s^{-1} = M^{-1} + s$.

A Green's function for M^{-1} has spectral decomposition $M(x, y) = \sum_n \frac{f_n(x) f_n^*(y)}{\lambda_n}$

then the the deformed operator is $M_s(x, y) = \sum_n \frac{f_n^*(y) f_n(x)}{\lambda_n + s}$ and

$$\log \frac{\det M^{-1}(\varphi)}{\det M^{-1}(\chi)} = -\int_0^\infty \mathrm{d}s \int \mathrm{d}^4 x \, M_s(\varphi; x, x) - M_s(\chi; x, x)$$

In the planar wall approx. and up to a cutoff in tangential momentum:

$$\log \frac{\det M^{-1}(\varphi_b)}{\det M^{-1}(0)} = -\int_0^\infty \mathrm{d}s \int_{-\infty}^\infty \mathrm{d}z \int \mathrm{d}^3\mathbf{x} \int_0^\infty \mathrm{d}k \, \frac{k^2}{2\pi^2} \operatorname{tr}\left(M_{s,\mathbf{k}}(\varphi_b; z, z) - M_{s;\mathbf{k}}(0; z, z)\right)$$

12. The tadpole contributions

The tadpoles give contributions to order $\hbar$ and are:

$$\Pi_{\hat{\Phi}}(\varphi_b; z)\,\varphi_b(z) = \frac{1}{2}\int \frac{\mathrm{d}^3\mathbf{k}}{(2\pi)^3}\left[6\,\lambda\,\varphi_b(z) + 15\,\lambda_6\,\varphi_b^3(z)\right]\mathscr{M}_{\hat{\Phi};\mathbf{k}}(\varphi_b; z, z),$$

$$\Pi_{(A_\mu,G)}(\varphi_b; z)\,\varphi_b(z) = \frac{1}{2}\int \frac{\mathrm{d}^3\mathbf{k}}{(2\pi)^3}\,\mathrm{tr}\left(\mathscr{M}_{(A_\mu,G);\mathbf{k}}(\varphi_b; z, z)\,\frac{\partial\mathscr{M}^{-1}_{(A_\mu,G);\mathbf{k}}(\varphi)}{\partial\varphi}(z)\bigg|_{\varphi_b}\right),$$

$$\Pi_{(\bar{\eta},\eta)}(\varphi_b; z)\,\varphi_b(z) = -2\zeta\,g^2\int \frac{\mathrm{d}^3\mathbf{k}}{(2\pi)^3}\,\mathscr{M}_{(\bar{\eta},\eta);\mathbf{k}}(\varphi_b; z, z)\,\varphi_b(z).$$

they are computed directly once the Green's functions are available and allow immediate comparison with the CW case however they remain cutoff dependent.

13.1. Results

Gradient effects on the total tadpole functions: intermittent curves represent the old result, while the solid line includes the gradient corrections. The bottom row displays the results after renormalizing and including the tree-level contributions respectively.

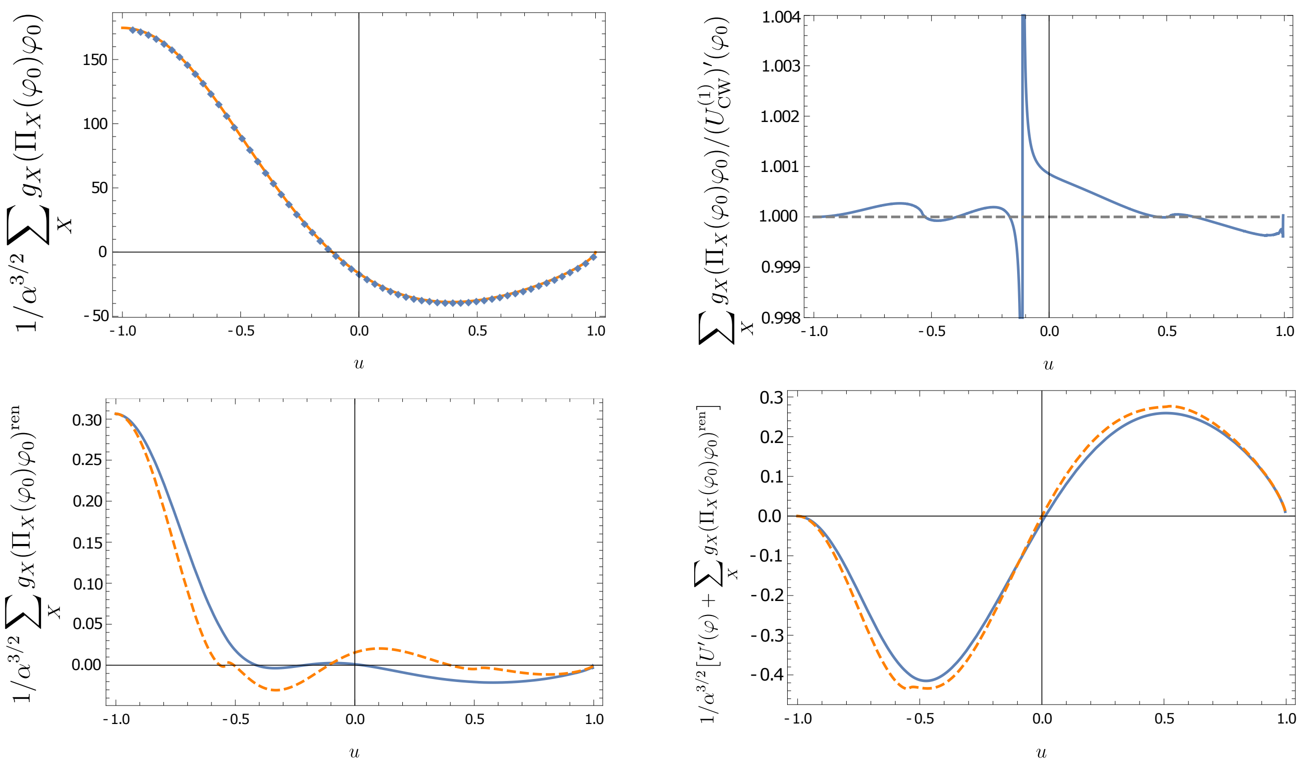

13.2. Results

Sector	Value $[\times\alpha^{-3/2}]$	Value$/((\mathscr{B}^{(0)}+\mathscr{B}^{(1)\mathrm{ren}})/V)$ [%]
$g_{\hat{\Phi}}B_{\hat{\Phi}}^{(1)\mathrm{ren,grad}}/V$	0.00139	0.29
$g_{(\bar{\eta},\eta)}B_{(\bar{\eta},\eta)}^{(1)\mathrm{ren,grad}}/V$	0.0000748	0.016
$g_{(A_4,G)}B_{(A_4,G)}^{(1)\mathrm{ren,grad}}/V$	0.00332	0.70
$\sum_X g_X B_X^{(1)\mathrm{ren,grad}}/V$	0.00479	1.0

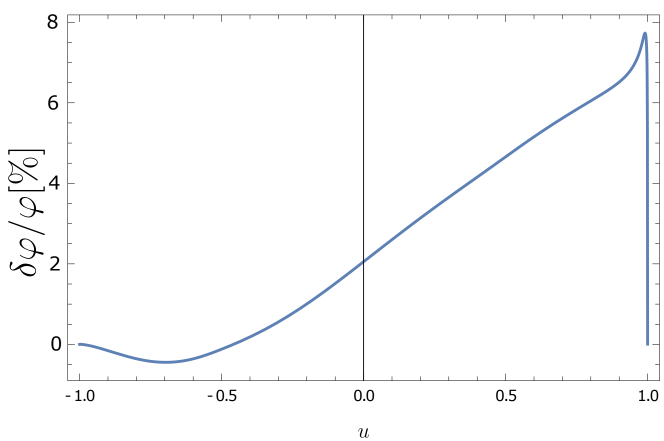

13.2. Results

Sector	Value $[\times\alpha^{-3/2}]$	Value$/((\mathscr{B}^{(0)}+\mathscr{B}^{(1)\mathrm{ren}})/V)$ [%]
$g_{\hat{\Phi}} B_{\hat{\Phi}}^{(1)\mathrm{ren,grad}}/V$	0.00139	0.29
$g_{(\bar{\eta},\eta)} B_{(\bar{\eta},\eta)}^{(1)\mathrm{ren,grad}}/V$	0.0000748	0.016
$g_{(A_4,G)} B_{(A_4,G)}^{(1)\mathrm{ren,grad}}/V$	0.00332	0.70
$\sum_X g_X B_X^{(1)\mathrm{ren,grad}}/V$	0.00479	1.0

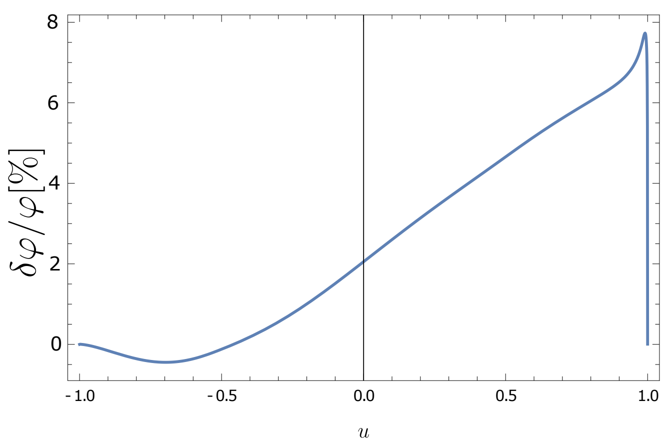

Contribution	Value $[\alpha^{-3/2}]$
$(\mathscr{B}^{(0)}+\mathscr{B}^{(1)\mathrm{ren}})/V$	0.473
$\mathscr{B}^{(2)\mathrm{ren}}/V$	-0.000345
$(\mathscr{B}^{(0)}+\mathscr{B}^{(1)\mathrm{ren}}+\mathscr{B}^{(2)\mathrm{ren}})/V$	0.474

14. Conclusions and Outlook

- The exponents for the decay rate for this model are computed with corrections coming from gradients of the background using a self-consistent prescription, indicating contributions from gradients comparable to 1-loop.
- A numerical treatment has been developed to compute the quantities involved which can be applied to other cases.
- We renormalize the theory to 1-loop through the use of the CW potential and a gradient expansion.

14. Conclusions and Outlook

- The exponents for the decay rate for this model are computed with corrections coming from gradients of the background using a self-consistent prescription, indicating contributions from gradients comparable to 1-loop.
- A numerical treatment has been developed to compute the quantities involved which can be applied to other cases.
- We renormalize the theory to 1-loop through the use of the CW potential and a gradient expansion.

Ongoing...

- Looking into more realistic models. Get closer to the Standard Model.
- Using the gradient expansion methods to obtain generic estimates of the gradient sizes.
- Curved space-times and early cosmology scenarios...

14. Conclusions and Outlook

- The exponents for the decay rate for this model are computed with corrections coming from gradients of the background using a self-consistent prescription, indicating contributions from gradients comparable to 1-loop.
- A numerical treatment has been developed to compute the quantities involved which can be applied to other cases.
- We renormalize the theory to 1-loop through the use of the CW potential and a gradient expansion.

Ongoing...

- Looking into more realistic models. Get closer to the Standard Model.
- Using the gradient expansion methods to obtain generic estimates of the gradient sizes.
- Curved space-times and early cosmology scenarios...

15. Gradient expansion to estimate gradient effects

The techniques used for wave-function renormalization can be used to estimate gradient effects roughly without a full numerical study.

Contribution	Numerical [$\alpha^{3/2}$]	Gradient Est. [$\alpha^{3/2}$]
$B_{\phi}^{(1)\mathrm{hom}}$	0.00478	0.009
$B_{\phi}^{(1)\mathrm{ren\,grad}}$	0.00139	0.0005
$B_{A_\mu,G}^{(1)\mathrm{ren\,grad}}$	0.00332	0.0014

We can observe how the gradient contributions depend on the parameters of the theory. There exist regions where gradients may become larger than homogeneous 1-loop effects.

Backup slides

A.1. Quantum Tunneling

Tunneling Phenomena

- Energetically forbidden regions are accessed in QM through tunneling.
- Probabilities of excitation are exponentially suppressed.

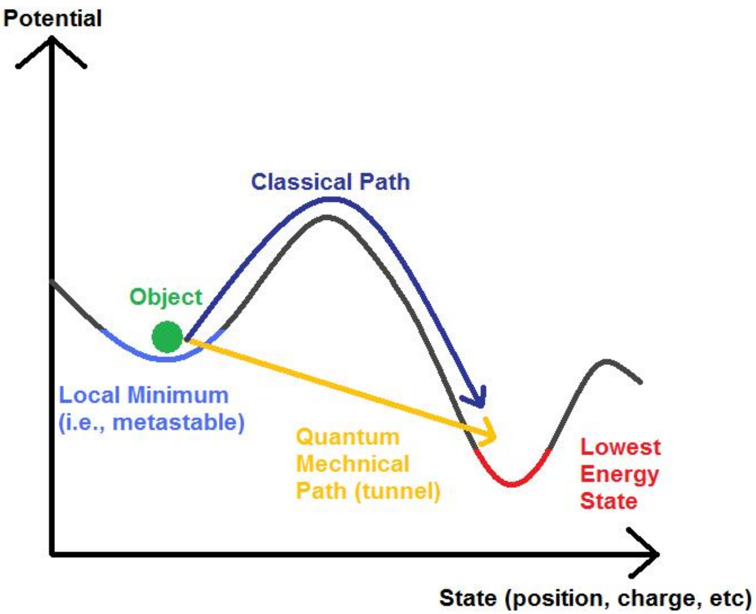

A.1. Quantum Tunneling

Tunneling Phenomena

- Energetically forbidden regions are accessed in QM through tunneling.
- Probabilities of excitation are exponentially suppressed.

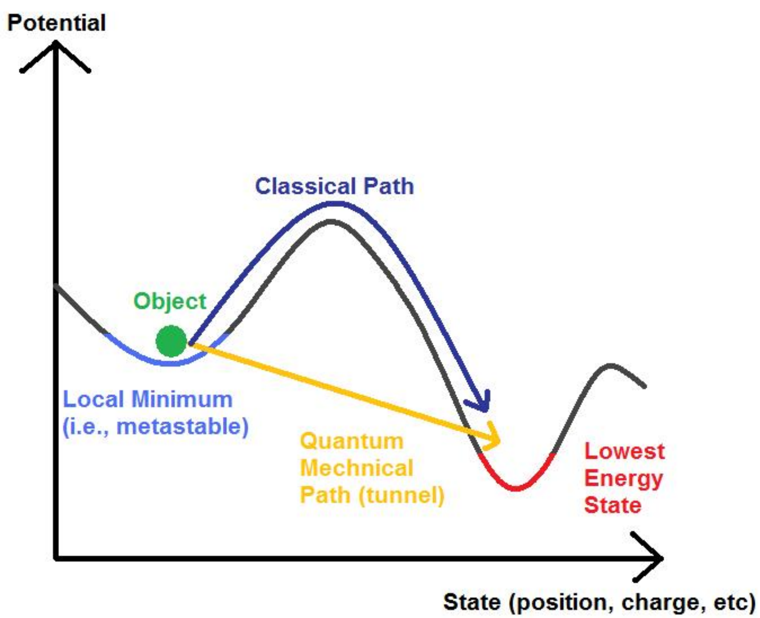

Vacuum state decay

- The expectation value of a field at tree-level corresponds to a local minimum.
- A theory with more than one local minimum presents different vacuum sectors.
- They can be connected by specific Euclidean solutions of the classical e.o.m..

A.2. The Questions

Are quantities computed using effective potentials gauge independent?

[Jackiw, 1974]
[Andreassen et al., 2014]

The effective potential is generally not gauge-independent, unless the quantities rely solely on extremal points.

(see [Nielsen, 1975, Aitchison and Fraser, 1984], [Metaxas and Weinberg, 1996, Lalak et al., 2016], [Endo et al., 2017, Plascencia and Tamarit, 2016].)

A.2. The Questions

Are quantities computed using effective potentials gauge independent?

[Jackiw, 1974]
[Andreassen et al., 2014]

The effective potential is generally not gauge-independent, unless the quantities rely solely on extremal points.

(see [Nielsen, 1975, Aitchison and Fraser, 1984], [Metaxas and Weinberg, 1996, Lalak et al., 2016], [Endo et al., 2017, Plascencia and Tamarit, 2016].)

A.2. The Questions

Are quantities computed using effective potentials gauge independent?

[Jackiw, 1974]
[Andreassen et al., 2014]

The effective potential is generally not gauge-independent, unless the quantities rely solely on extremal points.

(see [Nielsen, 1975, Aitchison and Fraser, 1984], [Metaxas and Weinberg, 1996, Lalak et al., 2016], [Endo et al., 2017, Plascencia and Tamarit, 2016].)

- **How to deal with gauge fields using these methods?**

A.2. The Questions

Are quantities computed using effective potentials gauge independent?

[Jackiw, 1974]
[Andreassen et al., 2014]

The effective potential is generally not gauge-independent, unless the quantities rely solely on extremal points.

(see [Nielsen, 1975, Aitchison and Fraser, 1984], [Metaxas and Weinberg, 1996, Lalak et al., 2016], [Endo et al., 2017, Plascencia and Tamarit, 2016].)

- **How to deal with gauge fields using these methods?**
- **How big are the contributions to the rate coming from radiative corrections and gradient effects?**

A.2. The Questions

Are quantities computed using effective potentials gauge independent?

[Jackiw, 1974]
[Andreassen et al., 2014]

The effective potential is generally not gauge-independent, unless the quantities rely solely on extremal points.

(see [Nielsen, 1975, Aitchison and Fraser, 1984], [Metaxas and Weinberg, 1996, Lalak et al., 2016], [Endo et al., 2017, Plascencia and Tamarit, 2016].)

- **How to deal with gauge fields using these methods?**
- **How big are the contributions to the rate coming from radiative corrections and gradient effects?**
- **Are higher loop corrections to decay rates over inhomogeneous backgrounds gauge dependent?**

A.3. Details for the computation of the bounce

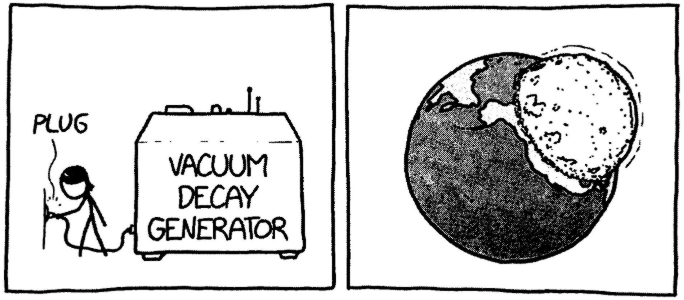

Found in "How To: Absurd Scientific Advice for Common Real-World Problems"
by Randall Munroe author of XKCD.com Comics

Boundary conditions for the bounce

$$t = \pm\infty, \phi(t, \mathbf{x}) = \phi_{fv} \qquad \text{and} \qquad |\mathbf{x}| \to \infty, \phi \to \phi_{fv}$$

Find a bounce solution for tuned CW-potential, center the wall and extend values to infinity.

Conclusions from the previous studies:

- Scalar loops increase B and cause faster decay.
- Fermion loops decrease B and prolong the decay.

Parameters used for the current study:

$$\alpha = 2 \quad \lambda = -2.02546 \quad \beta = \frac{1}{2} \quad g = \frac{1}{2}$$

A.4. The Devils

- **Tuning the potential** One must ensure the validity of the thin wall approximation by picking potentials that present degenerate vacua.
- **Tuning the potential** To obtain finite functional determinants one requires degeneracy at the CW-level.

A.4. The Devils

- **Tuning the potential** One must ensure the validity of the thin wall approximation by picking potentials that present degenerate vacua.
- **Tuning the potential** To obtain finite functional determinants one requires degeneracy at the CW-level.
- **Renormalizing** The model is not renormalizable without introducing higher-dim ops.
- **Renormalizing** The CW-potential allows to extract coupling counterterms, the wavefunction one is obtained through a mixed representation gradient expansion.

A.4. The Devils

- **Tuning the potential** One must ensure the validity of the thin wall approximation by picking potentials that present degenerate vacua.
- **Tuning the potential** To obtain finite functional determinants one requires degeneracy at the CW-level.
- **Renormalizing** The model is not renormalizable without introducing higher-dim ops.
- **Renormalizing** The CW-potential allows to extract coupling counterterms, the wavefunction one is obtained through a mixed representation gradient expansion.
- **Numerical obstacles:** Corrections need sampling in two dimensions for numerical integrals with interpolation steps in between (one iteration needs around 15k sec with 6 cores., it takes long)
- **Numerical obstacles:** A large region in $|\mathbf{k}|$ must be scanned.

A.5. Extracting the negative and the zero modes

A negative mode contributes an imaginary part and allows for the tunneling interpretation, for thin wall:

$$\lambda_0 = -\frac{3}{R^2}$$

The fluctuation operator contains 0 modes corresponding to certain symmetries of the bounce solution, e.g. the location of the wall.

Functional determinants require these to be extracted such 0 modes. The determinants that appear in the presentation include this contributions as pre-factors via integration of their collective coordinate.

$$\hbar B^{(1)}_{\hat{\Phi};\mathrm{dis}} = \frac{\mathrm{i}\pi\hbar}{2} - \frac{\hbar}{2}\log\left(\frac{(V\mathscr{T})^2\alpha^5}{4|\lambda_0|}\left(\frac{B}{2\pi\hbar}\right)^4\right)$$

A.6. The slide for Feynman fans

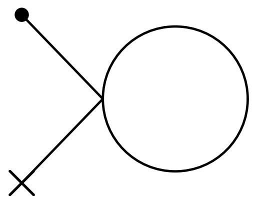

(a) First type of contributions from $\hat{\Phi}$.

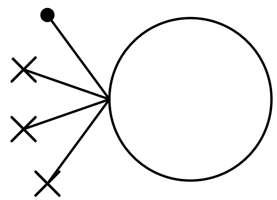

(b) Second tadpole type contribution from $\hat{\Phi}$

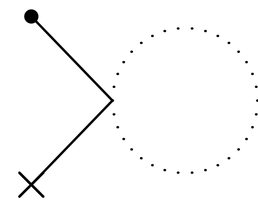

(c) Tadpole contribution coming from the ghost fields $\bar{\eta}, \eta$.

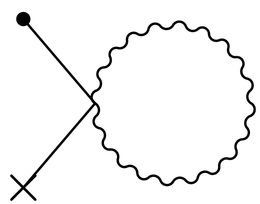

(d) Tadpole contributions from the gauge field components A_1, A_2, A_3 parallel to the bubble wall.

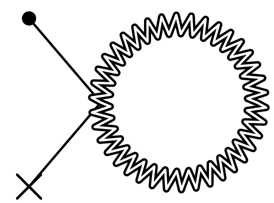

(e) Tadpole contribution coming from the coupled sector of A_4, G.

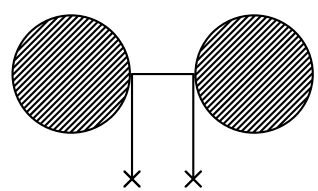

(f) Dumbbell diagram corresponding to the $B^{(2)}$ corrections coming from the improvements to the initial bounce.

× represents background insertions

● represents fluctuations around φ_b

A.7. Quest for a solution III: larger **k** values

Numerical perturbative solution

For a value of $|\mathbf{k}|$, solve diagonals numerically for $M^{(0)}(u,u')$ (orange dashed) and iterate for corrections (solid blue).

Compute quantities of interest such as determinants and tadpole contributions by reconstructing functions for a range of $|\mathbf{k}|$.

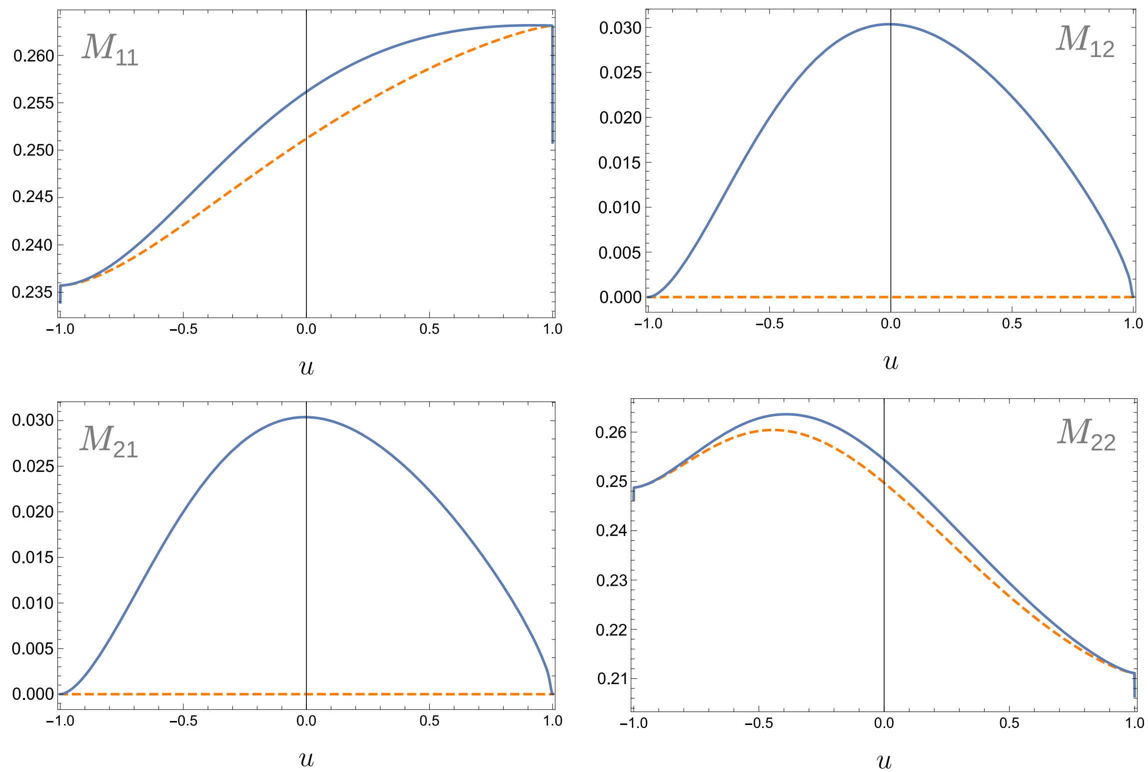

A.8. Renormalization

Counter terms for the theory are found through homogeneous terms coming from CW analogue computations

$$\mathscr{L}_{\rm ct}[\varphi] = \frac{1}{2}\delta Z(\partial\varphi)^2 + \frac{\delta\alpha}{2}\varphi^2 + \frac{\delta\lambda}{4}\varphi^4 + \frac{\delta\lambda_6}{8}\varphi^6 + \frac{\delta\lambda_8}{16}\varphi^8.$$

the homogeneous term for the scalar field for example, looks like:

$$I_1 \equiv \frac{\hbar}{2}\int_{B_\Lambda}\frac{\mathrm{d}^3\mathbf{k}}{(2\pi)^3}\int_{-\infty}^{\infty}\frac{\mathrm{d}k_4}{2\pi}\log\frac{k_4^2+\mathbf{k}^2+U''(\phi)}{k_4^2+\mathbf{k}^2+U''(\phi_{fv})},$$

which together with similar terms for the other sectors allow to determine the coupling counter-terms. We impose a *MS*-scheme on our toy model.

A.9. Wave-function renormalization

One adds and subtracts a kernel obtained from a gradient expansion to the effective action, as well as a counter term for just the divergences:

$$\begin{aligned}\Gamma|_{\text{ren}} \supset \frac{1}{2}\mathrm{tr}\int_0^{\Lambda_s^2} ds \int d^4x\,(\mathscr{M}_{\varphi_b,s}(x,x) - \mathscr{M}^{\text{hom}}_{\varphi_b,s}(x,x) + K_s(x)(\partial\varphi_b)^2) \\ - \int d^4x\,(V^{\text{ren}}_{\text{CW}}(\varphi_b) - V^{\text{ren}}_{\text{CW}}(v)) - \frac{1}{2}\int d^4x(\partial\varphi_b)^2 \\ - \frac{1}{2}\int d^4x\,(K(x) + \delta Z)(\partial\varphi_b)^2.\end{aligned}$$

This ensures the integrand in the first line only has terms that are finite when to cutoff is taken to infinity.

A.9. Wave-function renormalization

One adds and subtracts a kernel obtained from a gradient expansion to the effective action, as well as a counter term for just the divergences:

$$\begin{aligned}\Gamma|_{\text{ren}} \supset \frac{1}{2}\mathrm{tr}\int_0^{\Lambda_s^2} ds \int d^4x\,(\mathscr{M}_{\varphi_b,s}(x,x) - \mathscr{M}^{\text{hom}}_{\varphi_b,s}(x,x) + K_s(x)(\partial\varphi_b)^2)\\ -\int d^4x\,(V^{\text{ren}}_{\text{CW}}(\varphi_b) - V^{\text{ren}}_{\text{CW}}(v)) - \frac{1}{2}\int d^4x(\partial\varphi_b)^2\\ -\frac{1}{2}\int d^4x\,(K(x) + \delta Z)(\partial\varphi_b)^2.\end{aligned}$$

[Chan, 1985], [Cheyette, 1985]
[Gaillard, 1986], [Henning et al., 2016]

This ensures the integrand in the first line only has terms that are finite when to cutoff is taken to infinity. K is then obtained from an expansion of the form:

$$\Gamma \supset -\frac{1}{4}\int \mathrm{d}^4x\frac{\mathrm{d}^4p}{(2\pi)^4}\left(\frac{\partial^2\Delta_{A,\mu\mu}}{\partial p_\rho\partial p_\sigma}\partial_\rho\partial_\sigma m_A^2 + \frac{\partial^2\Delta_G}{\partial p_\rho\partial p_\sigma}\partial_\rho\partial_\sigma m_G^2\right);\quad \Delta_X = \frac{1}{p^2+m_X^2}$$

where an expansion like the one below was used

$$\mathrm{tr}\log\tilde{\mathscr{M}}^{-1}_{(A_\mu,G,p)}(x) = \mathrm{tr}\log\tilde{\mathscr{M}}^{-1}_{0(A_\mu,G,p)} - \mathrm{tr}\sum_{m=1}^{\infty}\frac{(-1)^m}{m}\left(\tilde{\mathscr{M}}_{0(A_\mu,G,p)}(\tilde{\mathscr{M}}^{-1}_{1(A_\mu,G,p)} + \tilde{\mathscr{M}}^{-1}_{2(A_\mu,G,p)})\right)^m$$

A.10. Contact with Phenomenology

A possible UV completion

Our theory although picks specific higher dimensional operators, it can be thought of as an effective field theory coming from a UV-theory having heavy Dirac fermions Ψ, χ, in which Ψ is a gauge singlet and χ has charge -1,:

$$\mathscr{L}_{\text{heavy}} = -y\bar{\Psi}\Phi\chi + h.c.$$

One-loop diagrams have interactions $\lambda_{2m}|\Phi|^{2m}$ with

$$\lambda_{2m} \sim \frac{y^{2m}}{16\pi^2 M^{2(m-2)}}$$

At the benchmark point, this means each higher order interaction after 6 will be suppressed by a factor of $1/10$ for a coupling y within the perturbative regime.

$$\left.\frac{\lambda_n|\Phi|^{2m}}{\lambda_6|\Phi|^6}\right|_{|\Phi|^2=\alpha=2} = \left(\frac{4\pi}{y^2}\right)^{2(m-3)} .$$

A.11. Results

Gradient effects on the tadpole functions are shown per field, the dashed line is the CW-result while the solid line includes gradient corrections:

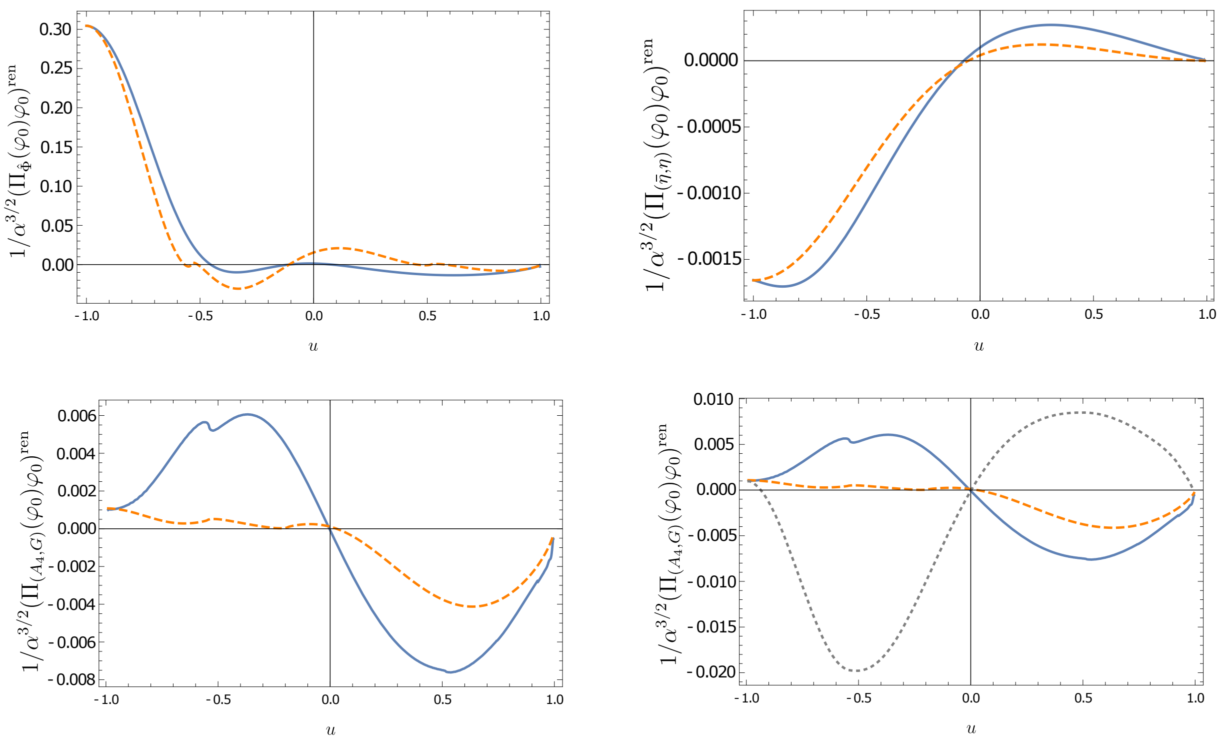

The scalar field suffers the largest corrections due to the background, followed by the $A_4 - G$ sector.